Density-functional theory for vacancies in hard-sphere crystals

Benito Groh

FOM Institute for Atomic and Molecular Physics, Kruislaan 407, 1098 SJ Amsterdam, The Netherlands

The equilibrium vacancy concentration in solids can be computed from density-functional theory (DFT) if allowance is made for density profiles with less than one particle per lattice site. For the fundamental-measure theory (FMT), this approach predicts reasonably small vacancy concentrations in hard sphere crystals, in contrast to earlier DFTs. Using an asymptotic analysis of the FMT functional, it is shown that the number of vacancies depends exponentially on the distance to the close packing density, as expected from heuristic arguments. The prefactor of the exponential is calculated for three recently suggested variants of the theory, using density profiles obtained from a quasifree minimization. Extrapolation of the asymptotic behavior to the melting density yields good agreement with other estimates and computer simulation results.

PACS number(s): 61.20.Gy, 61.50.Ah, 61.72.−y

I. INTRODUCTION

In the last two decades density-functional theory (DFT) has been established as a unified description of the liquid and solid phases of simple model systems like the hard-sphere fluid. Although based on results of liquid state theory such as correlation functions, DFT predicts the location of the freezing transition as well as the solid structure with satisfactory accuracy. Among the large number of DFT versions developed for hard spheres [1], the newest and most successful is the fundamental-measure theory (FMT) of Rosenfeld and co-workers [2,3]. While the general structure of the FMT functional has deep connections to scaled particle theory and Percus-Yevick theory, its detailed form has recently been rederived and slightly modified by enforcing the correct behavior in the limit of zero-dimensional cavities that can hold only one particle [4,5]. Thus it is not too surprising that FMT performs extremely well in describing the hard-sphere crystal in which particles essentially move in small cages formed by their neighbors. We recently showed that FMT reproduces such subtleties as the deviation of the density peaks from a Gaussian shape and the next-to-leading term of the free energy in the close packing limit in fair agreement with computer simulations [6]. The latest FMT version [5] actually gives more accurate free energies for the solid than for the liquid, for which it reduces to the Percus-Yevick result.

In this work we address another subtle effect, which may be important for the determination of elastic constants [7–9] and high precision free energy measurements [10,11], namely, the small but finite equilibrium concentration of vacancies in the hard-sphere crystal. This means that on average there is less than one particle per lattice site. This situation is included in the DFT formalism in a natural way by taking into account non-normalized density peaks. However, when applied to the Ramakrishnan-Yussouff DFT [12,13], which represents the first and simplest successful theory of freezing, the relaxation of the normalization condition produces unphysically high vacancy concentrations [14]. But also more sophisticated variants which employ weighted densities suffer from the same shortcoming [15].

Motivated by this failure, a different approach to the vacancy problem within DFT has been suggested [16]. The basic idea is to insert a density profile $\rho(\mathbf{r})$ with a vacancy at a fixed lattice site into the functional and to account for the configurational entropy of the vacancy by an additional term. For the Lennard-Jones fluid the results seemed indeed quite reasonable, while the hard-sphere vacancy concentration comes out about five orders of magnitude too small. A similar approach has been applied to films of hard disks in a periodic potential modeling absorbed monolayers [17]. However, in our opinion this method is not well justified. The value of the functional at a nonequilibrium density distribution with a localized vacancy has no physical meaning and it is not necessarily related to the free energy of vacancy formation.

It has been claimed [18,19] that FMT is capable of predicting the correct vacancy concentration if non-normalized peaks are used. But the corresponding short paragraph in Ref. [19] is, in our opinion, rather obscure and incorrect. In the present paper we therefore carefully study the vacancy problem within FMT. We find that indeed it yields the correct order of magnitude for the number of vacancies as well as the correct density dependence in the close packing limit.

II. FUNDAMENTAL MEASURE THEORY

We first recapitulate the basic equations of the fundamental-measure functional for a one-component hard-sphere system. One defines a set of weighted densities $n_\alpha(\mathbf{r})$ which follow from the density profile $\rho(\mathbf{r})$ as

$$n_\alpha(\mathbf{r}) = \int d^3r' \, w_\alpha(\mathbf{r}-\mathbf{r}')\rho(\mathbf{r}') \tag{1}$$

with weight functions w_α whose range is the particle radius $\sigma/2$. Their explicit form is

$$w_3(\mathbf{r}) = \Theta(\sigma/2 - r), \tag{2}$$

$$w_2(\mathbf{r}) = \delta(\sigma/2 - r), \tag{3}$$

$$\mathbf{w}_{V2}(\mathbf{r}) = \hat{\mathbf{r}}\delta(\sigma/2 - r), \tag{4}$$

$$\mathbf{w}_{T2}(\mathbf{r}) = \hat{\mathbf{r}}_i \otimes \hat{\mathbf{r}}_j \delta(\sigma/2 - r), \tag{5}$$

where $\hat{\mathbf{r}}$ is a unit vector, Θ the Heaviside step function, and $\mathbf{w}_{V2}$ and $\mathbf{w}_{T2}$ give rise to vector and tensor weighted densities, respectively. The excess part of the free energy functional is expressed as

$$\beta F_{ex}[\rho(\mathbf{r})] = \int d^3r \sum_{i=1}^{3} \phi_i(n_\alpha(\mathbf{r})) \tag{6}$$

where the free energy densities ϕ_i are functions of the weighted densities only and are given as

$$\phi_1 = -\frac{n_2}{\pi\sigma^2}\ln(1-n_3), \quad \phi_2 = \frac{n_2^2 - \mathbf{n}_{V2}^2}{2\pi\sigma(1-n_3)},$$

$$\phi_3 = \frac{f_3(n_\alpha)}{(1-n_3)^2}. \tag{7}$$

The best choice for the function f_3 has been subject to some discussion recently. We will consider three variants here. An empirical correction to the original FMT [2],

$$f_3^{FMT1} = \frac{(n_2^2 - \mathbf{n}_{V2}^2)^3}{24\pi n_2^3}, \tag{8}$$

suggested by Rosenfeld et al. [19], enabled the first successful description of the solid phase. A new derivation of FMT based on the requirement of correctly describing the zero-dimensional limit yielded [4]

$$f_3^{FMT2} = \frac{9}{8\pi}\det \mathbf{n}_{T2} \tag{9}$$

as an approximation to a more complicated result which could not be expressed in terms of weighted densities. In Ref. [6] we showed that FMT2 is superior to FMT1 when applied to high density crystals. A third version,

$$f_3^{FMT3} = \frac{3}{16\pi}[\mathbf{n}_{V2}\cdot\mathbf{n}_{T2}\cdot\mathbf{n}_{V2} - n_2\mathbf{n}_{V2}^2 - \text{tr}(\mathbf{n}_{T2}^3) + n_2\,\text{tr}(\mathbf{n}_{T2}^2)], \tag{10}$$

has recently been found by Tarazona after reexamination of the mentioned derivation [5]. Finally, the complete functional is obtained by adding the ideal gas contribution,

$$\beta F_{id}[\rho(\mathbf{r})] = \int d^3r \rho(\mathbf{r})[\ln\rho(\mathbf{r})\lambda^3 - 1], \tag{11}$$

where λ is the thermal de Broglie wavelength.

In a solid the density profile consists of identical density peaks $\rho_\Delta(\mathbf{r})$ centered at the lattice sites $\mathbf{R}$:

$$\rho(\mathbf{r}) = \sum_{\mathbf{R}} \rho_\Delta(\mathbf{r}-\mathbf{R}), \tag{12}$$

which implies a corresponding decomposition of the weighted densities:

$$n_\alpha(\mathbf{r}) = \sum_{\mathbf{R}} n_\Delta^{(\alpha)}(\mathbf{r}-\mathbf{R}). \tag{13}$$

III. CALCULATION OF THE VACANCY CONCENTRATION

While in a perfect crystal the individual peaks are normalized to 1, the existence of vacancies can be incorporated into the DFT by allowing for a different normalization:

$$\int d^3r\rho_\Delta(\mathbf{r}) = \frac{N}{N_s} = \eta_0 = 1 - x_v, \tag{14}$$

where N and N_s are the number of particles and lattice sites, η_0 is the average occupancy of the sites, and x_v the vacancy concentration. Note that in this approach the vacancies are spread over the whole system in thermodynamic equilibrium and not localized at specific sites. The vacancy concentration also enters the functional via the lattice constant, since for fixed bulk density $\rho_b = N/V$ the nearest neighbor distance is $R = R_0\eta_0^{1/3}$, where R_0 is the nearest neighbor distance in the corresponding perfect crystal [$R_0 = (\sqrt{2}/\rho_b)^{1/3}$ for the fcc lattice assumed here]. By minimizing with respect to all $\rho_\Delta(\mathbf{r})$ irrespective of their normalization, but under the constraint of fixed ρ_b, the equilibrium vacancy concentration can be determined.

Under the assumption of Gaussian density peaks

$$\rho_\Delta(r) = \eta_0\left(\frac{\alpha}{\pi}\right)^{3/2}e^{-\alpha r^2}, \tag{15}$$

this has been carried out before [14] using the Ramakrishnan-Yussouff DFT, which historically was the first to describe successfully the freezing of hard spheres [12,13]. However, within this approximation, which corresponds to a second-order expansion of the functional around the fluid state, a far too high vacancy concentration ($\sim 10\%$) was found at the melting density. We have confirmed this result and extended the calculations to higher densities. It is found that the occupancy η_0 increases and crosses unity at $\rho_b^* = \rho_b\sigma^3 = 1.405$, implying more than one particle per site on average. Even worse, the close packing limit of the Ramakrishnan-Yussouff theory is lost if this additional freedom is taken into account. That means that the peak width $\Delta = 1/\sqrt{\alpha}$ still decreases with increasing ρ_b but no longer goes to zero when the maximum possible density $\rho_b^* = \sqrt{2}$ is approached [6]. In Ref. [15] a number of other DFT versions have been subjected to the same procedure. None of them yielded a reasonably small order of magnitude for the vacancy concentration at its respective melting density.

On the other hand, it has been claimed that FMT is capable of predicting the correct value of x_v [18,19]. We attempted to confirm this by numerical calculation of x_v. Unfortunately this was prevented by its smallness, which leads to numerical problems during the minimization because the very weak dependence of the functional on x_v in the interesting region is lost in numerical noise due to rounding errors. But in the following we present an asymptotic analysis of the problem near the close packing limit, along the lines of our earlier investigation of the perfect crystal [6], which shows that the FMT result for x_v is indeed in agreement with the physical expectation.

We assume a general, spherical symmetric density profile, with the scaling form

$$\rho_\Delta(r) = \frac{\eta_0}{a^3}\rho_0\left(\frac{r}{a}\right) \quad \text{with} \quad \int d^3s\,\rho_0(s) = 1, \quad (16)$$

where $a = R - \sigma$ is the free distance between sites, which tends to zero in the close packing limit. Its relation to the free distance a_0 of a defect-free crystal with the same bulk density is

$$a = (\sigma + a_0)\eta_0^{1/3} - \sigma = a_0 - \frac{1}{3}x_v(\sigma + a_0) + O(x_v^2\sigma). \quad (17)$$

We now adopt the strategy of minimizing first with respect to x_v for fixed ρ_b (i.e., fixed a_0) and fixed profile $\rho_0(s)$, assuming that a_0/σ, a/σ, and x_v are small quantities. Afterward the optimum profile shape $\rho_0(s)$ follows by a second minimization. The leading contribution to the ideal free energy is

$$\beta F_{id}/N = 4\pi\int_0^\infty ds\,s^2\rho_0(s)[\ln\rho_0(s) - 1] - 3\ln(a_0/\lambda)$$
$$+ x_v\sigma/a_0 + \cdots. \quad (18)$$

The dots denote terms of order $(x_v\sigma/a_0)^2$ that will turn out to be neglegible. As shown in detail in Ref. [6], the weighted densities $n_\Delta^{(\alpha)}(\mathbf{r})$ have nontrivial values only in a small range of width proportional to a around $r = \sigma/2$ and can be expanded in powers of a for fixed $t = (r - \sigma/2)/a$. For the two scalar weighted densities one finds ($\delta = a/\sigma$)

$$n_\Delta^{(3)}(t) = \eta_0[n_{30}(t) + n_{31}(t)\delta + \cdots], \quad (19)$$

$$n_\Delta^{(2)}(t) = \frac{\eta_0}{a}[n_{20}(t) + n_{21}(t)\delta + \cdots], \quad (20)$$

with

$$n_{30}(t) = 4\pi\left(\Theta(-t)\int_0^{-t} ds\,s^2\rho_0(s) + \int_{|t|}^\infty ds\,s\rho_0(s)(s - t)\right), \quad (21)$$

$$n_{31}(t) = 2\pi\int_{|t|}^\infty ds\,s\rho_0(s)(t^2 - s^2), \quad (22)$$

$$n_{20}(t) = 2\pi\int_{|t|}^\infty ds\,s\rho_0(s), \quad (23)$$

$$n_{21}(t) = -2tn_{20}(t). \quad (24)$$

In any coordinate system with its z axis aligned with $\mathbf{r}$ the vector weighted density is

$$\mathbf{n}_\Delta^{(V2)}(t) = \hat{\mathbf{r}}\frac{\eta_0}{a}[n_{20}(t) + n_{21}(t)\delta + \cdots] \quad (25)$$

and the tensor weighted density

$$\mathbf{n}_\Delta^{(T2)} = \begin{pmatrix} n_\Delta^{(11)} & 0 & 0 \\ 0 & n_\Delta^{(11)} & 0 \\ 0 & 0 & n_\Delta^{(33)} \end{pmatrix} \quad (26)$$

with

$$n_\Delta^{(11)}(t) = -2\frac{\eta_0\delta}{\sigma}n_{31}(t) + \cdots, \quad (27)$$

$$n_\Delta^{(33)}(t) = n_\Delta^{(2)}(t) - 2n_\Delta^{(11)}(t). \quad (28)$$

Contributions from different lattice sites must be transformed to a common reference frame before they are added to the total vector and tensor weighted densities.

The spatial integration in Eq. (6) over the Wigner-Seitz cell of the lattice is now split into two parts (see Fig. 6 in Ref. [6]): region A where the total weighted densities are dominated by the contributions from one site, and region B around the midpoints between two neighboring sites, where both sites contribute to the weighted densities. Power laws for the δ dependence of the individual contributions $\Phi_{ij} = N^{-1}\int_j d^3r\,\phi_i$ with $i = 1,2,3$ and $j = A,B$ are given in Ref. [6]. Here we are interested in the x_v dependence of the dominant terms.

Let us first consider

$$\Phi_{1A} = -\frac{N_s}{N}\int_A d^3r\frac{n_\Delta^{(2)}(r)}{\pi\sigma^2}\ln[1 - n_\Delta^{(3)}(r)]. \quad (29)$$

Extending the integration region to a full spherical shell introduces no error in the leading term, so that one has

$$\Phi_{1A} = -\int_{-\infty}^\infty dt\,n_{20}(t)\ln[1 - \eta_0 n_{30}(t)] + O(\delta)$$

$$= 1 + \frac{x_v}{1 - x_v}\ln x_v, \quad (30)$$

where $\partial n_{30}/\partial t = n_{20}$ and $n_{30}(t \to \infty) = 0$, $n_{30}(t \to -\infty) = 1$ have been used. Thus the leading term is independent of the profile and nonanalytical at $x_v = 0$. It can be shown that the $O(\delta)$ term from Φ_{1A} exactly cancels with the corresponding term from Φ_{2A} for all x_v when the integration region is a full sphere. However, the missing caps in the directions to the 12 nearest neighbors give rise to an additional $O(\delta)$ correction Φ_{1A}^{cap}. Taking into account all contributions up to $O(\delta)$ we have in FMT3

$$\frac{\beta F_{ex}}{N} = 1 + x_v\ln x_v + \Phi_{2B}^{00} + x_v\Phi_{2B}^{01}$$

$$+ \left(\frac{a_0}{\sigma} - \frac{x_v}{3}\right)(\Phi_{1B}^{00} + \Phi_{2B}^{10} + \Phi_{3B}^{00} + \Phi_{1A}^{cap}) \quad (31)$$

where

$$\Phi_{ij}^{nm} = \frac{\partial^{n+m}}{\partial a^n\partial x_v^m}\Phi_{ij}\Big|_{a=0,x_v=0} \quad (32)$$

and terms of the orders a_0^2, $a_0 x_v$, $x_v^2 \ln x_v$ have been neglected. [Neglected terms of $O(\delta^2)$ will be important if they behave as $c_1 + c_2 x_v (\ln x_v)^2$ for small x_v. There are indications that this is indeed the case for the region A contributions when Gaussian profiles are used, but not for the actual minimum profile which ultimately decays faster than a Gaussian.] The only change in FMT2 is that Φ_{3B}^{00} drops out because $\Phi_{3B} \sim \delta^3$ in this version [6]. In FMT1 $\Phi_{3B} \sim \delta^{-1}$ is the dominant term. As shown in Ref. [6] it is minimized for profiles $\rho_0(s)$ with a cutoff at $s = 1/2$, for which region B (and the missing caps of region A) do not exist. For such profiles only the first two terms in Eq. (32) remain.

Minimization of the total free energy with respect to x_v for fixed a_0 results in

$$x_v = \exp\left(K - \frac{\sigma}{a_0} \right) \qquad (33)$$

with $K^{FMT1} = -1$, $K^{FMT2} = -1 - \Phi_{2B}^{01} + (\Phi_{1B}^{00} + \Phi_{2B}^{10} + \Phi_{1A}^{cap})/3$, and $K^{FMT3} = K^{FMT2} + \Phi_{3B}^{00}/3$. Equation (33) is our central result.

The exponential decay of the vacancy concentration is in agreement with the following estimate. The free energy of vacancy formation is approximately the work pV/N required to enlarge the crystal by one lattice site against the external pressure, which leads to $x_v \simeq \exp(-\beta p/\rho_b)$ [20]. Together with the asymptotic form $\beta p/\rho_b = \sigma/a_0 + \cdots$ for the equation of state, predicted by cell theory as well as FMT, Eq. (33) is recovered.

Since x_v is exponentially smaller than a_0/σ, all x_v dependent terms can be neglected for the calculation of the optimum peak shape, i.e., the asymptotic peak shape $\rho_0(s)$ is exactly the one calculated before for the perfect crystal. We recall that it is a step function in FMT1, while in both FMT2 and FMT3 one obtains the same function, which very much resembles a Gaussian but decays faster for large s.

The calculation of the constant K is described in the Appendix and yields $K^{FMT2} = 0.39$ and $K^{FMT3} = 0.92$. Extrapolation of Eq. (33) to the melting density $\rho_b^* = 1.04$ gives $x_v^{FMT1} = 3.5 \times 10^{-5}$, $x_v^{FMT2} = 1.4 \times 10^{-4}$, and $x_v^{FMT3} = 2.4 \times 10^{-4}$, all in reasonable agreement with the molecular dynamics result [20], but in contrast to the previous FMT1 estimate 3.5×10^{-8} [19] which in our opinion is wrong. Figure 1 compares the vacancy concentration according to Eq. (33) for all three versions with simulation data [20,21]. We emphasize that the lines are extrapolations of the asymptotic behavior and differ from the results of the full DFT, which could not be determined for the reasons given above. Therefore we hesitate to draw conclusions on the relative quality of the different versions of the theory. The almost perfect FMT3 value at melting is probably fortuitous. Bowles and Speedy [21] have measured the volume and surface area of cavities in simulated crystals with one (nonequilibrium) vacancy. From these data they derived the equilibrium vacancy concentrations shown in Fig. 1. If one uses their formulas with the asymptotic equation of state of Alder *et al.* [22] one recovers Eq. (33) for $a_0 \rightarrow 0$ with the value $K = 0.33$, which is quite close to the FMT2 result.

We remark that if the functional is evaluated for a density profile with a localized vacancy, as suggested by McRae *et*
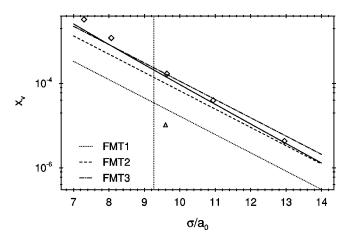

FIG. 1. Vacancy concentration as function of the free distance a_0. The lines for the three FMT versions are extrapolations of the asymptotic behavior for $a_0 \rightarrow 0$, the diamonds [20] and the full line [21] are simulation results, and the triangle is a theoretical estimate by Schaaf and Reiss [23]. The vertical line denotes the melting density; crystals on the left of this line are metastable.

al. [16], in FMT2 and FMT3 the leading contribution to the free energy difference between the crystal with and without the vacancy is the ideal free energy per particle $-3 \ln a_0/\lambda$ which, together with the configurational entropy $\sim x_v \ln x_v$, leads to the wrong prediction $x_v(a_0 \rightarrow 0) \sim a_0^3$, corresponding to a much too slow decay of x_v.

APPENDIX: CALCULATION OF THE CONSTANT K

The integral over the missing spherical caps of region A that have been included in Eq. (29) is

$$\delta \Phi_{1A}^{cap} = -24\pi \int_{R/2}^{\infty} dr \, r^2 \left(1 - \frac{R}{2r} \right) \phi_1(n_\Delta^{(\alpha)}(r)). \qquad (A1)$$

By using the substitution $t = (r - \sigma/2)/a$ and Eqs. (19) and (20) we get

$$\Phi_{1A}^{cap} = 12 \int_{1/2}^{\infty} dt \, (t - 1/2) \, n_{20}(t) \ln[1 - n_{30}(t)], \qquad (A2)$$

where η_0 has been set to 1 because only the leading term is needed.

For the integration over region B scaled variables $\rho = \rho'^2/(a\sigma)$ and $z = z'/a$ are used where (ρ', z', ϕ') is a cylindrical coordinate system centered at the midpoint between

two sites and with its polar axis directed toward one of them. For spherical density distributions all integrands are independent of ϕ'. One easily finds

$$\Phi_{1B}^{00} = -12 \int_0^\infty dz \int_0^\infty d\rho [(n_{20}^+ + n_{20}^-)\ln(1 - n_{30}^+ - n_{30}^-) - n_{20}^- \ln(1 - n_{30}^-)] \tag{A3}$$

with $n_\alpha^\pm = n_\alpha(t_\pm) = n_\alpha(1/2 + \rho \mp z)$. The second term is subtracted because it was already included in Φ_{1A}.

For Φ_{2B} the vectors $\mathbf{r}_\pm$ pointing to the neighboring sites are written as

$$\mathbf{r}_\pm = \begin{pmatrix} \rho' \cos\phi' \\ \rho' \sin\phi' \\ z' \pm R/2 \end{pmatrix}. \tag{A4}$$

The angle γ between the directions to the two sites is determined by $\cos\gamma = \hat{\mathbf{r}}_+ \cdot \hat{\mathbf{r}}_- = -1 + 8\rho\delta + O(\delta^2)$ so that [see Eqs. (20) and (25)]

$$n_2^2 - \mathbf{n}_{V2}^2 = \frac{4\eta_0^2}{a^2} \{ n_{20}(z_+)n_{20}(z_-) + \delta[n_{20}(z_+)n_{21}(z_-) + n_{20}(z_-)n_{21}(z_+) - 4\rho n_{20}(z_+)n_{20}(z_-)] \} \tag{A5}$$

with

$$z_\pm = \frac{r_\pm - \sigma/2}{a} = t_\pm - \rho(1 + \rho \pm 2z)\delta + \cdots = t_\pm + u_\pm\delta + \cdots. \tag{A6}$$

Expanding the $O(\delta^0)$ term to first order in x_v one obtains

$$\Phi_{2B}^{01} = -24 \int_0^\infty dz \int_0^\infty d\rho \frac{n_{20}^+ n_{20}^-}{(1 - n_{30}^+ - n_{30}^-)^2}. \tag{A7}$$

The $O(\delta)$ term for $x_v = 0$ is

$$\Phi_{2B}^{10} = 24 \int_0^\infty dz \int_0^\infty d\rho \left(\frac{-n_{20}^+ n_{20}^-(u_- n_{20}^- + u_+ n_{20}^+) + n_{31}^+ + n_{31}^-}{(1 - n_{30}^+ - n_{30}^-)^2} + \frac{n_{20}^+ n_{20}'^- u_- + n_{20}^- n_{20}'^+ u_+}{1 - n_{30}^+ - n_{30}^-} \right) \tag{A8}$$

where $n_{20}'(t) = \partial n_{20}(t)/\partial t = -2\pi t\rho_0(t)$ and all weighted densities are evaluated at $t_\pm = 1/2 + \rho \mp z$.

Finally, after more lengthy algebra involving the transformation between the reference frames attached to $\mathbf{r}_+$ and $\mathbf{r}_-$, we find in FMT3

$$\Phi_{3B}^{00} = -36 \int_0^\infty dz \int_0^\infty d\rho \frac{n_{20}^+ n_{20}^-(n_{31}^+ + n_{31}^-)}{(1 - n_{30}^+ - n_{30}^-)^2}. \tag{A9}$$

Using the asymptotic profile determined in Ref. [6] numerical evaluation of Eqs. (A2), (A3), (A8), and (A9) gives the results for the constant K quoted in the main text. For comparison, one finds $K_{FMT2} = 0.55$ and $K_{FMT3} = 1.08$ for a Gaussian profile with optimized width.

[1] R. Evans, in *Fundamentals of Inhomogeneous Fluids*, edited by D. Henderson (Marcel Dekker, New York, 1992), Chap. 3, pp. 85–175.

[2] Y. Rosenfeld, Phys. Rev. Lett. **63**, 980 (1989).

[3] Y. Rosenfeld, in *New Approaches to Problems in Liquid State Theory*, Vol. 529 of *NATO Science Series*, edited by C. Caccamo, J.-P. Hansen, and G. Stell (Kluwer, Dordrecht, 1999), pp. 303–320.

[4] P. Tarazona and Y. Rosenfeld, Phys. Rev. E **55**, R4873 (1997).

[5] P. Tarazona, Phys. Rev. Lett. **84**, 694 (2000).

[6] B. Groh and B. Mulder Phys. Rev. E (to be published).

[7] M. Jarić and U. Mohanty, Phys. Rev. Lett. **58**, 230 (1987).

[8] D. Frenkel and A. Ladd, Phys. Rev. Lett. **59**, 1169 (1987).

[9] M. Bates and D. Frenkel Phys. Rev. E (to be published).

[10] S.-C. Mau and D. Huse, Phys. Rev. E **59**, 4396 (1999).

[11] S. Pronk and D. Frenkel, J. Chem. Phys. **110**, 4589 (1999).

[12] T. Ramakrishnan and M. Yussouff, Phys. Rev. B **19**, 2775 (1979).

[13] A. Haymet, J. Chem. Phys. **78**, 4641 (1983).

[14] G. Jones and U. Mohanty, Mol. Phys. **54**, 1241 (1985).

[15] R. Ohnesorge, Ph.D. thesis, Universität München, 1994 (unpublished).

[16] R. McRae, J. McCoy, and A. Haymet, J. Chem. Phys. **93**, 4281 (1990).

[17] L. Mederos, P. Tarazona, and G. Navascués, Phys. Rev. B **35**, 3384 (1987).

[18] Y. Rosenfeld, J. Phys.: Condens. Matter **8**, L795 (1996).

[19] Y. Rosenfeld, M. Schmidt, H. Löwen, and P. Tarazona, Phys. Rev. E **55**, 4245 (1997).

[20] C. Bennett and B. Alder, J. Chem. Phys. **54**, 4796 (1971).

[21] R. Bowles and R. Speedy, Mol. Phys. **83**, 113 (1994).

[22] B. Alder, W. Hoover, and D. Young, J. Chem. Phys. **49**, 3688 (1968).

[23] P. Schaaf and H. Reiss, J. Chem. Phys. **92**, 1258 (1990).